Comparison of 3-D Coupled Calculations and Measurements Concerning the Structural-Dynamic Behavior of Induction Furnaces Excited by Electromagnetic Forces

T. Bauer, J. Gschwilm, and G. Henneberger

***Abstract*—The main topics of the work are the improved three-dimensional structural-dynamic and acoustic calculation of induction furnaces and the investigation of the vibration modes of the structure, which are excited by the Lorentz forces and magnetic forces.**

Furthermore the numerical analysis will be compared to a experimental modal analysis of an induction furnace and to acoustic measurements in normal operating mode. These data are suitable to evaluate the quality of the mesh and the material parameters used for the calculation. This step is the basis for the evaluation of a method for further optimization research.

***Index Terms*—Acoustic noise, finite element method, Lorentz force, magnetic surface force, modal analysis.**

I. Introduction

THE REDUCTION of the acoustic noise caused by electromagnetic forces requires an exact knowledge of the mechanisms, which lead to the emission of sound. This implies a systematic investigation of the structure, which is done by a coupled calculation of the electromagnetic forces, the structural-dynamic oscillations and the acoustic noise in the surrounding media. Since the noise calculation depends on the solution quality of each calculation step, an evaluation of the reliability has to be chosen. According to previous works on the field of electromagnetics [1] the force calculation is considered to have an error lower than 5%. Therefore the focus is laid on the structural-dynamic calculation and the acoustic calculation. The calculation sequence to determine the sound emission is shown in Fig. 1.

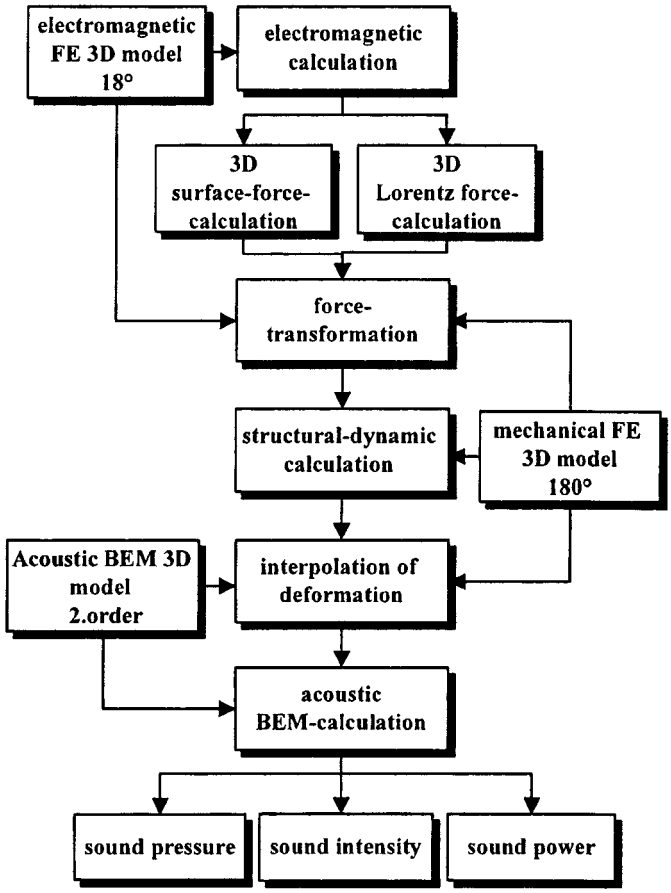

Fig. 1. Flow of calculation for the determination of the noise emission.

II. Electromagnetic Forces

The induction furnace consists of three main parts [2]. The inner part is the melt, which is kept in a cylindrical crucible. Coils are wrapped around the crucible and consist of a passive coil at each end of the active coil. Additionally the attachment of yokes around the circumference reduces the stray field and gives mechanical support to the coils. Only those parts have to be considered for the electromagnetic calculation. All other parts of the induction furnace can be considered as air due to their electromagnetic properties.

To determine the eddy currents and the time-harmonic forces, an edge based $\vec{A}$, $\vec{A}-\vec{T}$ approach is used, which achieves the highest accuracy [3]. The total force $\vec{f}_{\text{total}}$ acting on the application is composed of Lorentz force densities $\vec{f}$—in the areas with electric conductivity—and surface force densities $\vec{\sigma}$—at boundaries from low to high magnetic permeability. The current density $\vec{S}$ and the magnetic flux density $\vec{B}$ are derived from the electric vector potential $\vec{T}$:

$$\vec{S} = \operatorname{rot} \vec{T}, \tag{1}$$

Manuscript received June 5, 2000.

T. Bauer and G. Henneberger are with the Department of Electrical Machines, Aachen Institute of Technology, RWTH, Germany (e-mail: {bauer; henneberger}@rwth-aachen.de).

J. Gschwilm is with the Department Institute of Aerolasticity, DLR Göttingen, Germany (e-mail: Joerg.Gschwilm@dlr.de).

Publisher Item Identifier S 0018-9464(01)07839-6.

and the magnetic vector potential $\vec{A}$:

$$\vec{B} = \text{rot}\ \vec{A}. \tag{2}$$

The magnetic energy w and the magnetic properties β_i, of the applied materials can depend on the location (x, y, z), the magnetic flux density $\vec{B}$ and other variables:

$$\vec{f}_{\text{total}}(t) = \vec{S}(t) \times \vec{B}(t) + \sum_{i=1}^{m} \frac{\partial w}{\beta_i} \text{grad}(\beta_i). \tag{3}$$

The following equation reveals the Lorentz force density, which is equal to the first term of the right hand side of the previous equation:

$$\vec{f} = \frac{1}{2} \begin{pmatrix} S_y B_z e^{j(\varphi_{S,y}+\varphi_{B,z})} - S_z B_y e^{j(\varphi_{S,z}+\varphi_{B,y})} \\ S_z B_x e^{j(\varphi_{S,z}+\varphi_{B,x})} - S_x B_z e^{j(\varphi_{S,x}+\varphi_{B,z})} \\ S_x B_y e^{j(\varphi_{S,x}+\varphi_{B,y})} - S_y B_x e^{j(\varphi_{S,y}+\varphi_{B,x})} \end{pmatrix} e^{j2wt}. \tag{4}$$

Assuming that no hysteresis is present and that the behavior is time-invariant, the surface force $\vec{\sigma}$ can be written as:

$$\vec{\sigma}(t) = \{(h_{1n}(t) - h_{2n}(t))bn(t) - (w_1'(t) - w_2'(t))\} \cdot n_{\vec{12}}. \tag{5}$$

The flux density $b_n(t)$ in normal direction to the boundary, the magnetic field strengths $h_{1n}(t)$ and $h_{2n}(t)$ at each side of the boundary and the magnetic coenergies $w_1'(t)$ and $w_2'(t)$ have to be determined for the surface force calculation. The smallest symmetry of 18° is modeled and the forces are calculated in complex terms. The absolute values of the forces in cylindric coordinates are depicted in Table I. The surface forces upon the yokes have minor influence on the vibration level, for they only amount to 2% of the Lorentz forces. The forces are transformed to a mechanical model, which contains additional suspension parts and has different mesh densities.

III. Numerical and Experimental Modal Analysis

The applied element type is a brick shaped eight node element modeling the solid volumes, like the crucible, the coils and the yokes. Quadrilateral shell elements with rotational degrees of freedom are used to model the platform and the supporting beam. These element types increase the accuracy of the structural-dynamic calculation. The mesh consist of 95% eight node bricks and quadrilateral elements with nearly rectangular angles and an aspect ratio smaller than 3 (Fig. 2). Only 5% of the elements are six node prisms lying in the axis of the crucible. This small amount of prisms does not have great impact on the solution of the modal or structural-dynamic analysis. The modal shapes and the eigen-frequencies are determined according to the equation:

$$(\mathrm{K} - \lambda_{\mathbf{i}} \cdot \mathrm{M}) \cdot \Psi_{\mathbf{i}} = \mathbf{0}, \tag{6}$$

where

- K is the stiffness matrix,
- M the mass matrix,
- λ_i the ith eigen-value and
- Ψ_i the eigen-vector of the ith form.

TABLE I
Comparison of the Force Components in Cylindrical Coordinate System

	surface force / N	Lorentz force / N
all directions	930	43237
radial	869	42130
circumferential	40	0
axial	107	9722

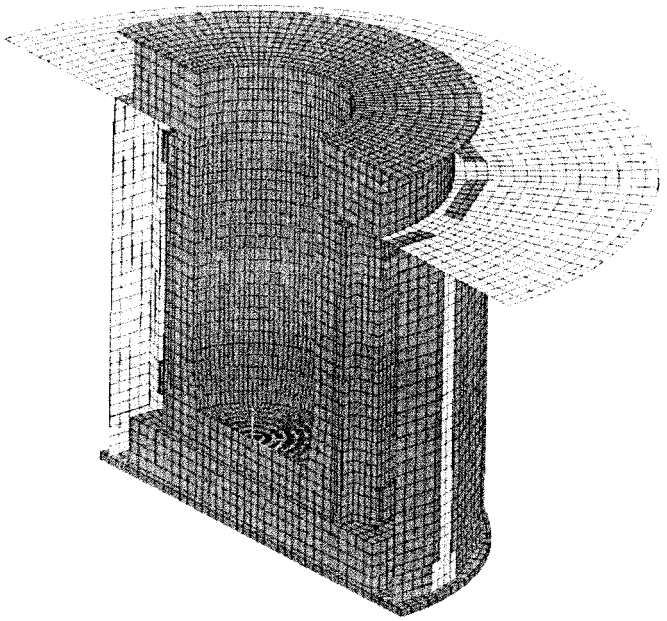

Fig. 2. The mechanical model for the modal analysis meshed with brick shaped elements.

TABLE II
The Measured Mode Shapes in Comparison to the Calculations (TR: Supporting Beam Radial; TU: Supporting Beam Circumferential; JR: Yoke Radial; JU: Yoke Circumferential)

frequency measured / Hz	frequency calculated / Hz	error / %	shape	damping / %	MPC / %
324,5	327	-0,77	JR 1.ord.	1.93	86,3
330,3	348	-5,36	JR 1.ord.	0,77	90,1
339,3	334	1,55	TU 1.ord.	0,17	86,6
367,3	348	5,25	JU 1.ord.	1,455	96,8
374,8	383	-2,17	TU 1.ord.	0,64	99,9
382,4	383	-0,16	TR 1.ord.	1,39	99,2
385,8	410	-6,26	TU 1.ord.	1,37	99,8
414,8	402	3,09	JU 1.ord.	1,59	99,8
419,2	408	2,67	TR 2.ord.	2,72	97,1
423,4	422	0,33	JR 1.ord.	2,3	99,3
432,8	433	-0,04	JR 1.ord.	0,35	99,6
433,1	411	5,10	TR 2.ord.	0,15	99,6
436,0	416	4,80	JU 1.ord.	1,91	99,9
442,6	433	2,16	JU 1.ord.	0,33	96,7
442,6	433	2,16	JR 1.ord.	0,35	99,6
446,6	434	2,83	TU 1.ord.	1,19	99,5
458,4	453	1,17	JR 1.ord.	1,44	97,2
459,7	438	4,73	TR 2.ord.	1,29	99,4
465,7	452	3.03	JU 1.ord.	1,35	98,9
486,6	489	-0,50	TU 1.ord.	3,79	99,7
512,7	508	0,91	TR 2.ord.	1,15	99,9

A frequency range of 20 to 800 Hz is calculated using the Block Lancos method to determine the eigen-vectors [4]. The numerical analysis is compared to an experimental analysis in Table II.

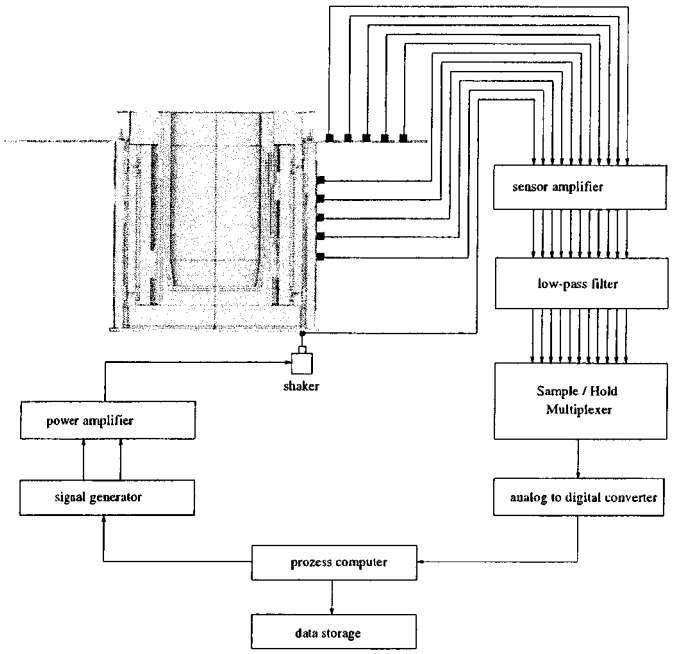

Fig. 3. Test setup for the experimental modal analysis.

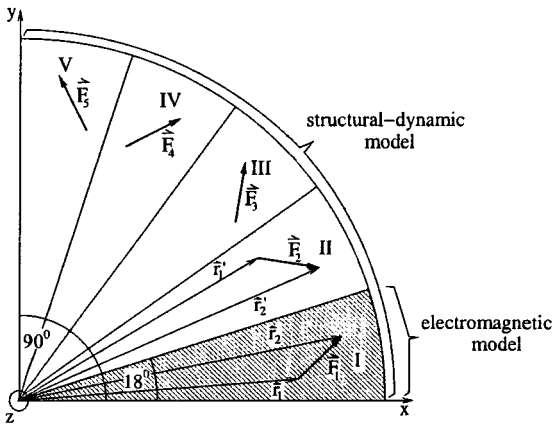

Fig. 4. Transformation of the forces from the electromagnetic to the mechanic model.

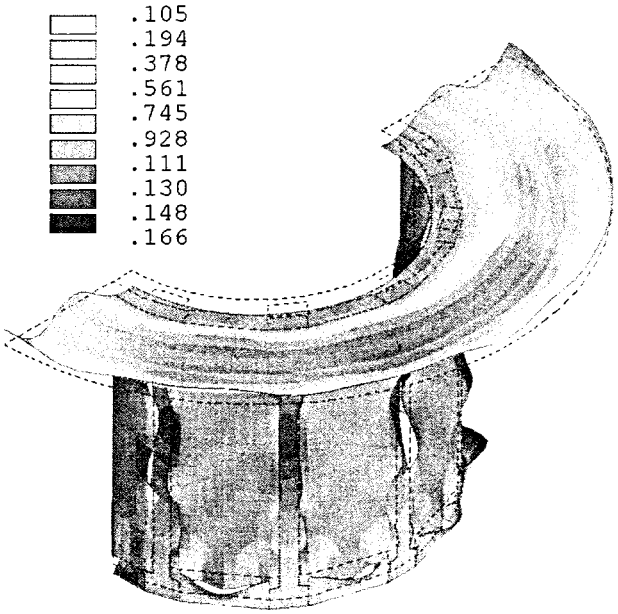

Fig. 5. Real part of the deformation (platform, supporting beam and rear plates/μm.

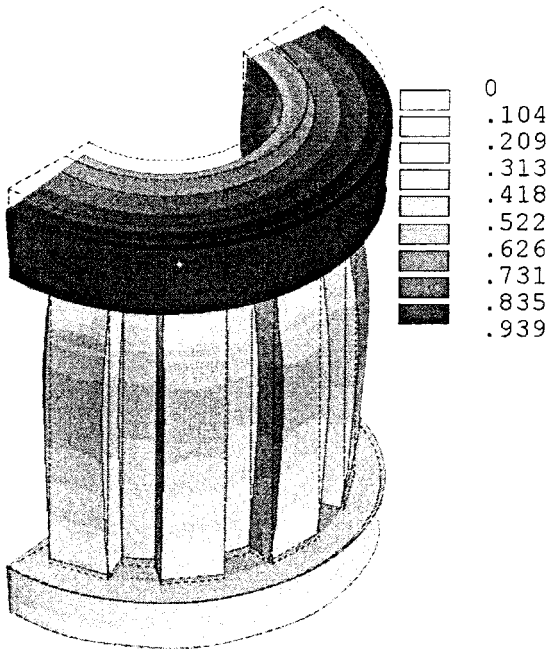

Fig. 6. Real part of the deformation (crucible, yoke and coils)/μm.

As depicted in Fig. 3 the measurement of the modes is done by the application of a shaker and a 12 channel front-end, controlled by a workstation. According to the nominal current frequency of 250 Hz, the acoustic frequency is 500 Hz. Therefore the upper frequency of the measurement range is set to 800 Hz. This is legal, because the Fourier analysis of the acoustic signal shows a distinct maximum at 500 Hz, whereas all other frequencies have levels, at least 15 dB lower than the maximum. According to Table II a good correspondence between measurements and calculation is achieved. The mode confidential value "MPC" shows, that all relevant modes with a reliability of at least 87% are identified and found in the numerical modal analysis. The maximum error of the identified eigen-frequency is smaller than 6%. All measured eigen-forms are also found in the calculation. Further on a harmonic vibration analysis is done on the basis of the calculated modes by using the mode superposition method. As input data for the structural-dynamic analysis the forces are transformed from the electromagnetic model to the mechanical model by a transformation algorithm. The program has to take into account, that transformation to a section with an even number means a rotation and reflection of the force. The sections with an odd number require only a rotation of the force as shown in Fig. 4. The result of the time-harmonic calculation is presented in Figs. 5 and 6. The platform and the plates between the supporting beams perform higher order modes with 3 respectively 4 maxima along the edges. The upper part of the furnace fulfills a toroidal movement around the upper end of the supporting beams. Due to the considerable large surface of this construction part and the phase coincidence, the upper part emits most of the sound power (Fig. 6).

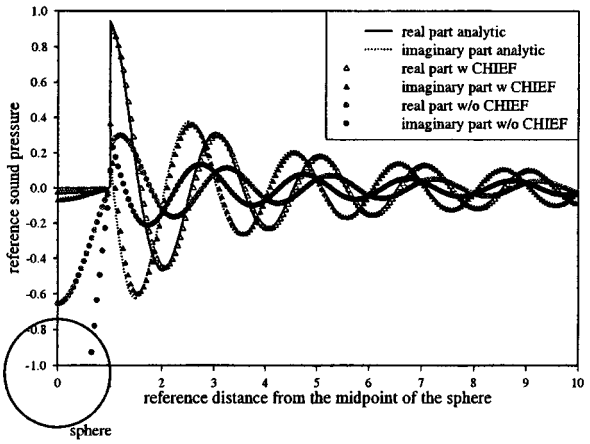

Fig. 7. The sound pressure of a pulsating sphere calculated with CHIEF.

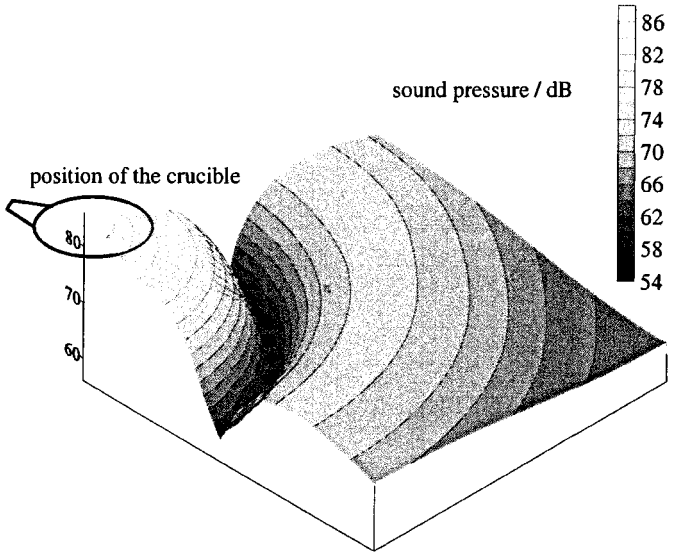

Fig. 8. Sound pressure 1.5 m above the platform (calculation).

IV. Numerical Noise Calculation

Another transformation provides the Boundary Element mesh with the correct surface velocities in order to calculate the sound pressure on top of the surface. The non uniqueness of the acoustic solution at the eigen-frequencies of the inner problem is solved by adding points to the system of equation, which are positioned in the inner structure of the acoustic model according to the CHIEF method [5]. The efficiency of the method is shown by the calculation of the sound pressure of a pulsating sphere at the first eigen-frequency (Fig. 7). In Fig. 8 the sound pressure on top of the platform is shown. Only by using the CHIEF method, the amplitude and the phase angle of the sound pressure are determined correctly. Measurements of the sound pressure were taken 1.5 m above the platform

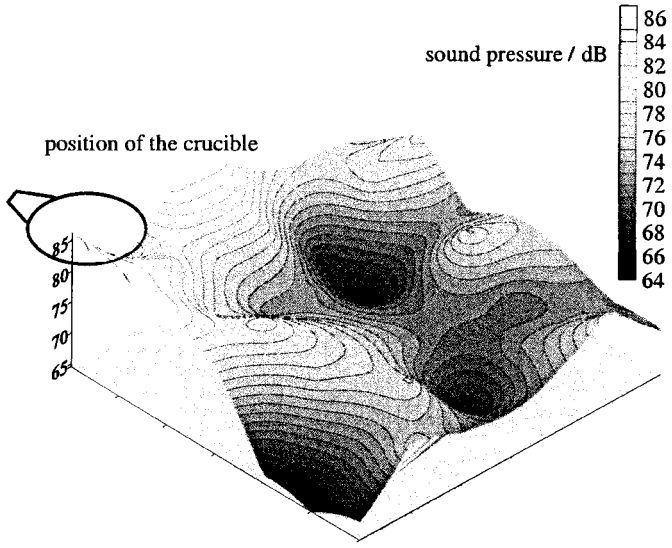

Fig. 9. Sound pressure 1.5 m above of the platform (measurement).

and with nominal electrical power. Due to reflections at other operation tools positioned on the platform, local maxima of the sound pressure occur in addition to the two maxima presented in the calculation. The measured sound pressure presented in Fig. 9, is in good accordance to the calculation depicted in Fig. 8.

V. Conclusion

This contribution presents an improved coupled 3D noise calculation. A comparison of the mode shapes and the sound field of the induction furnace shows good correspondence and proofs the method to be a suitable tool for further investigations in order to reduce the sound emission of induction furnaces and other electrical machines.

References

[1] D. Albertz, "Entwicklung numerischer Verfahren zur Berechnung und Auslegung elektromagnetischer Schienenbremssysteme," Ph.d. dissertation, Rheinisch-Westfälische Technische Hochschule, Aachen, 1999.

[2] T. Bauer, C. Monzel, and G. Henneberger, "Three-dimensional calculation of the acoustic behavior of electrical machines using boundary element method," in *Int. Seminar Vibrations and Acoustic Noise of Electric Machinery*, Bethune, 1998.

[3] T. Bauer, D. Albertz, and G. Henneberger, "Fully three dimensional method for the calculation of the time-harmonic magnetic, structural-dynamic and acoustic field of induction machines applied to an induction furnace," in *COMPUMAG*, Sapporo, Japan, 1999.

[4] R. Grimes, J. Lewis, and H. Simon, "A shifted block Lancos algorithm for solving sparse symmetric generalized eigenproblems," in *Journal Matrix Analysis Applications*: SIAM, 1994, vol. 15, pp. 228–272.

[5] A. Seybert, B. Soenarco, F. Rizzo, and D. Shippy, "An advanced computational method for radiation and scattering of acoustic waves in three dimensions," *Journal of the Acoustic Society of America (JASA)*, vol. 77, pp. 362–369, 1985.